Recent Charm Physics Results from LHCb

Liang Sun
Wuhan University
2022-12-10
全国第十九届重味物理和 CP 破坏研讨会

LHCb charm results since HFCPV2021

- Charm mixing & CPV
  - Mixing parameters in $D^0 \to h^- h^+$ [Phys. Rev. D**105** (2022) 092013]
  - Mixing parameters in $\overline{B} \to D^0 (\to K_S^0 \pi^+ \pi^-) \mu^- \overline{\nu}_\mu X$ [arXiv:2208.06512]
  - For CP-only results ($A_{CP}(h^+h^-)$, etc.), please see Jiesheng's talk
- Amplitude analyses of 3-body charm hadron decays
  - $D^+ \to \pi^+\pi^+\pi^-$ [arXiv:2208.03300], $D_s^+ \to \pi^+\pi^+\pi^-$ [arXiv:2209.09840]
  - $\Lambda_c^+ \to p K^- \pi^+$ [arXiv:2208.03261]
- Rare decays
  - $D^0 \to \mu^+\mu^+$ [LHCb-PAPER-2022-029]
- For other recent charm results (Ξ_{cc}^{++} related, etc.):

https://lhcbproject.web.cern.ch/Publications/LHCbProjectPublic/Summary_Charm.html

LHCb as a Charm factory

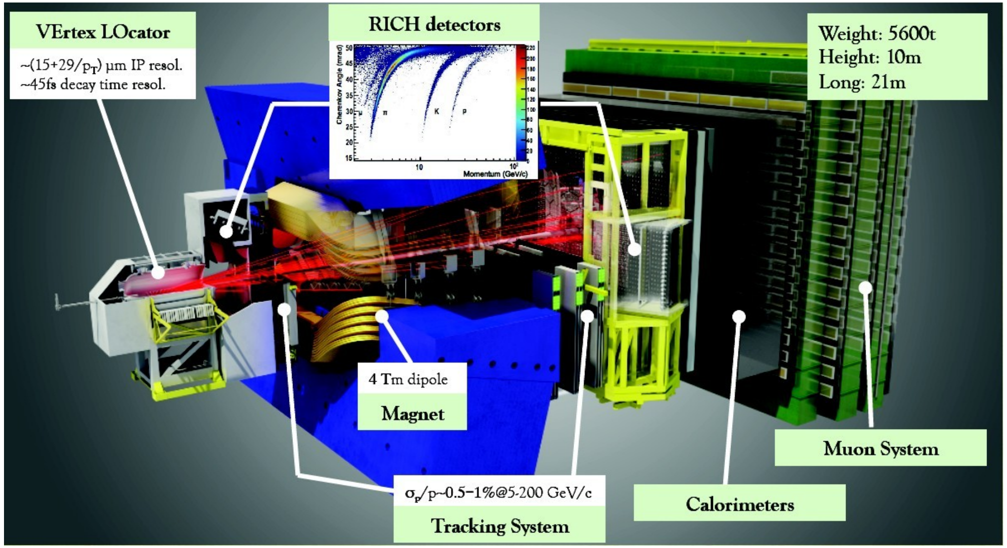

LHCb-CONF-2016-005

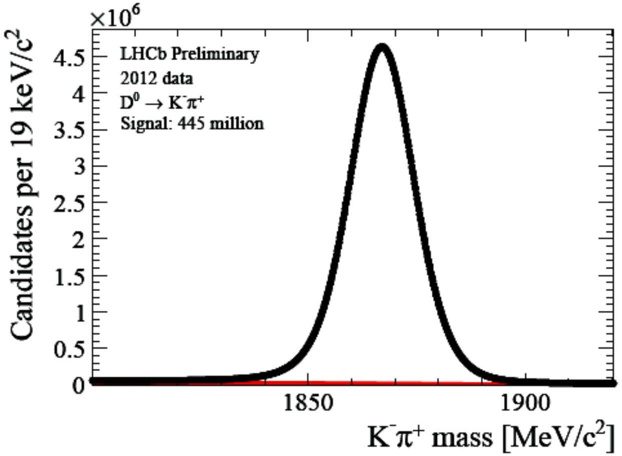

- LHCb acceptance: 2 < η < 5 (forward region)
- Large production cross-section

[JHEP 03 (2016) 159]

$$\sigma(pp \rightarrow c\bar{c}) = (2369 \pm 3 \pm 152 \pm 118)\,\mu b\,@\,13\,TeV$$

- More than 1 billion $D^0 \rightarrow K^-\pi^+$ collected by LHCb between 2011 and 2018
- Run2: Turbo stream from online reconstruction

[Comput. Phys. Commun. 208 (2016) 35]

D^0 production at LHCb

Two mechanisms of D^0 production

Independent data sample

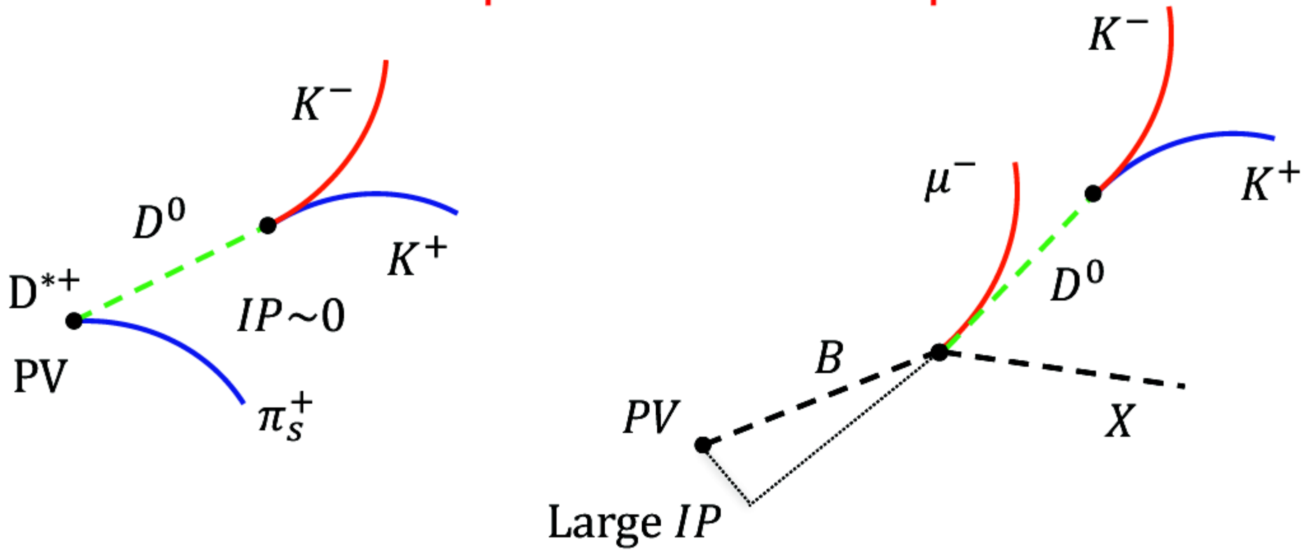

D^0 flavor tagging at LHCb

Experimentally we can tag D^0 flavour at production by means of the charge of the muon and the soft pion

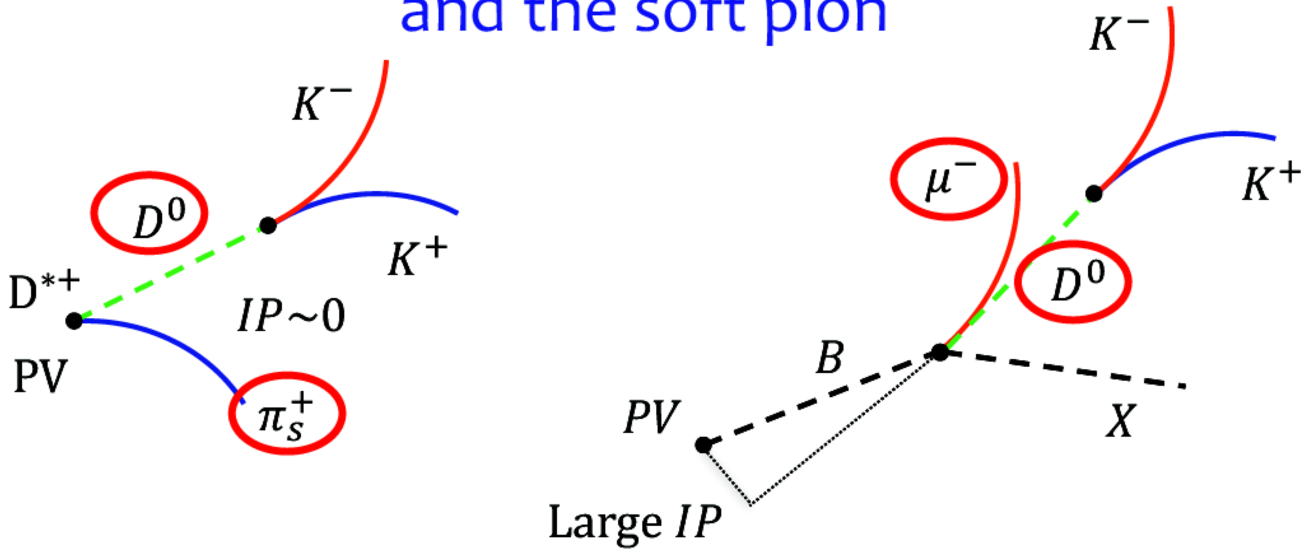

Mixing in neural D system

- Charm mixing – a well established fact
  - Mass eigenstates are related to their flavor eigenstates via $|D_{1,2}\rangle \equiv p|D^0\rangle \pm q|D^0\rangle$, with $|q|^2 + |p|^2 \equiv 1$
  - Mixing parameters based on the mass and width differences: $x \equiv (m_2 - m_1)/\Gamma$, $y \equiv (\Gamma_2 - \Gamma_1)/2\Gamma$, with D^0 decay width $\Gamma \equiv (\Gamma_2 + \Gamma_1)/2$

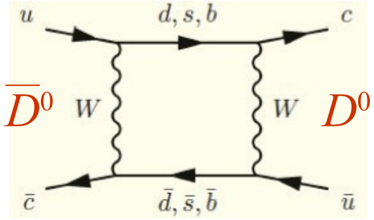

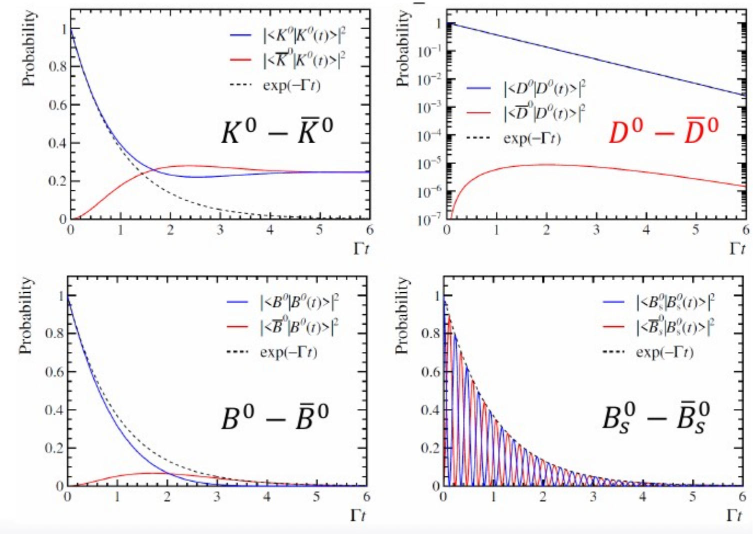

$$Prob(D^0 \to \bar{D}^0, t) = \left|\frac{q}{p}\right|^2 \frac{e^{-\Gamma t}}{2}(\cosh(y\Gamma t) - \cos(x\Gamma t))$$

Experimental knowledge of x and y [HFLAV and PDG]

System	x	y
$K^0 - \bar{K}^0$	-0.946 ± 0.004	0.99650 ± 0.00001
$D^0 - \bar{D}^0$	$(4.07 \pm 0.44)\times10^{-3}$	$(6.47 \pm 0.24)\times10^{-3}$
$B^0 - \bar{B}^0$	-0.769 ± 0.004	$(0.1 \pm 0.1)\times10^{-2}$
$B_s^0 - \bar{B}_s^0$	26.89 ± 0.07	$(12.9 \pm 0.6)\times10^{-2}$

[Phys. Rev. D**105** (2022) 092013]

Mixing parameters in $D^0 \to h^- h^+$

- Measuring the lifetime ratios of 2-body D^0 decays allows to constrain y

$$\frac{\tau(D^0 \to K^-\pi^+)}{\tau(D^0 \to f)} - 1 = y_{CP}^{f} - y_{CP}^{K\pi} \approx y\left(1 + \sqrt{R_D}\right)$$

$$y = \frac{\Gamma_2 - \Gamma_1}{2\Gamma} \approx 0.6\% \qquad R_D = \frac{\mathcal{B}(D^0 \to K^+\pi^-, t=0)}{\mathcal{B}(D^0 \to K^-\pi^+, t=0)} \approx 6\%$$

- $y_{CP}^{f} - y_{CP}^{K\pi}$ obtained by fitting to decay-time ratios:

$$R^f(t) = \frac{dN(D^0 \to f, t)}{dN(D^0 \to K^-\pi^+, t)} \propto e^{-(y_{CP}^{f} - y_{CP}^{K\pi})t/\tau_{D^0}} \frac{\varepsilon(f,t)}{\varepsilon(K^-\pi^+,t)}$$

- Using full 6 fb^{-1} Run2 data, D^0 from prompt $D^{*+} \to D^0 \pi^+_{tag}$ decays
- Biggest challenge: Equalizing time-dependent efficiencies in $R^f(t)$

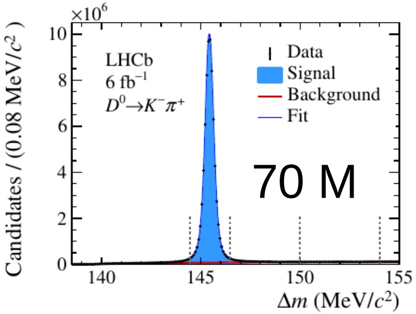

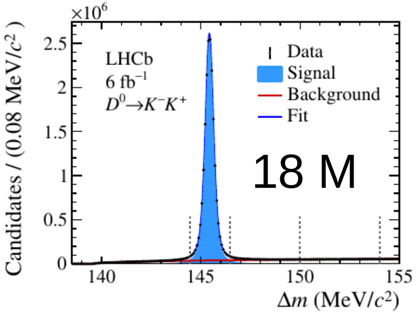

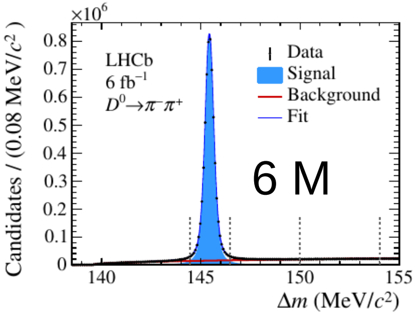

* Note: $y_{CP} - y_{CP}^{K\pi}$ was previously called y_{CP}. Term $-y_{CP}^{K\pi} \approx +0.4\times10^{-3}$ was included because of $D^0 \to K^-\pi^+ / D^0 \to K^+\pi^-$ mixing [JHEP03(2022)162].

[Phys. Rev. D**105** (2022) 092013]

Mixing parameters in $D^0 \to h^- h^+$

- The measured values are (slope of $R^f(t)$):

$$y_{CP}^{KK} - y_{CP}^{K\pi} = (7.08 \pm 0.30_{\text{stat}} \pm 0.14_{\text{sys}})\times 10^{-3}$$
$$y_{CP}^{\pi\pi} - y_{CP}^{K\pi} = (6.57 \pm 0.53_{\text{stat}} \pm 0.16_{\text{sys}})\times 10^{-3}$$

- Average: $y_{CP} - y_{CP}^{K\pi} = (6.96 \pm 0.26_{\text{stat}} \pm 0.13_{\text{sys}})\times 10^{-3}$

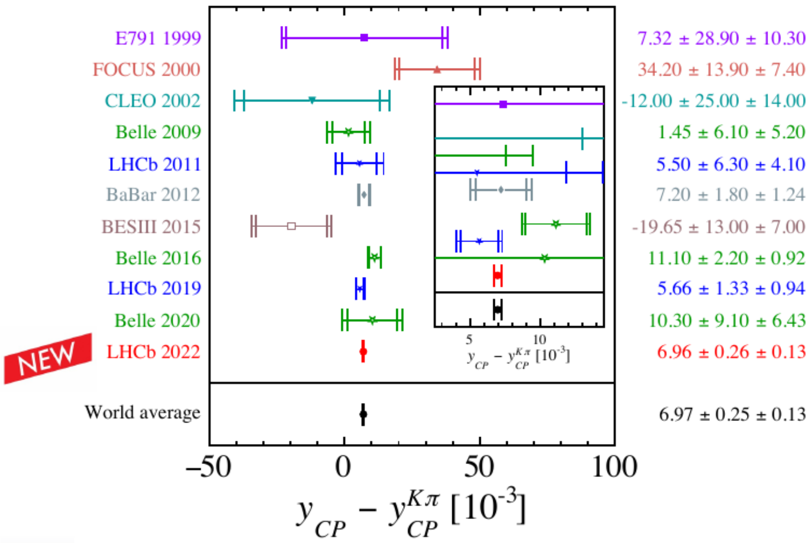

Four times more precise than previous world average value!

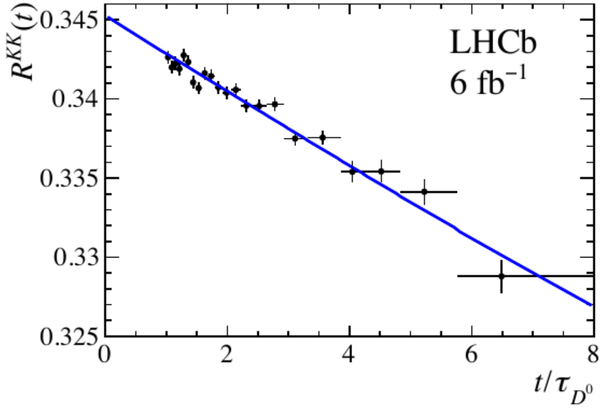

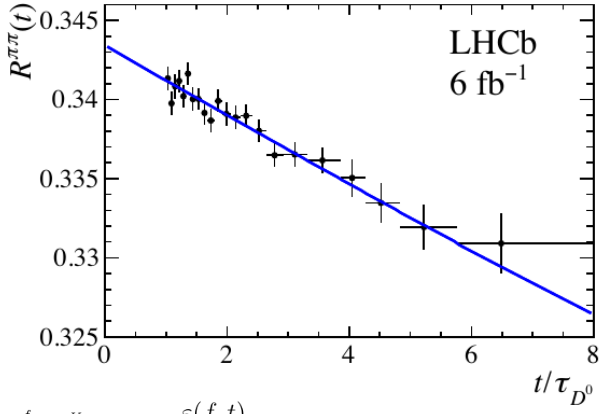

$$R^f(t) = \frac{N(D^0 \to f, t)}{N(D^0 \to K^-\pi^+, t)} \propto e^{-(y_{CP}^f - y_{CP}^{K\pi})\,t/\tau_{D^0}} \frac{\varepsilon(f,t)}{\varepsilon(K^-\pi^+,t)}$$

Mixing parameters in $\bar{B} \to D^0(\to K_S^0\pi^+\pi^-)\mu^-\bar{\nu}_\mu X$

- Using Run2 (5.4 fb^{-1}) data, D^0 from B decays & tagged by muon charge
- Complementary to prompt analysis [PRL 127 (2021) 111801], lower statistics (3.7 M vs. 31 M), but capable at small D^0 decay times
- Bin-flip method: model-independent approach, no need for modeling of Dalitz-plot efficiency & decay amplitudes
- Data binned in Dalitz-plot regions ±b, binning scheme chosen to have almost constant strong-phase differences between D^0 and $\bar{D}^0$ amplitudes

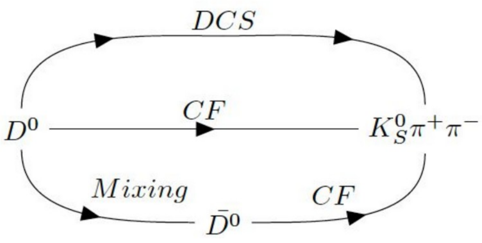

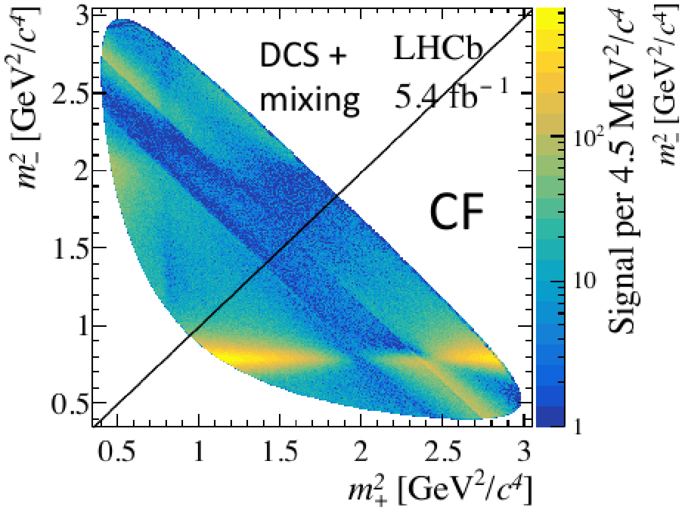

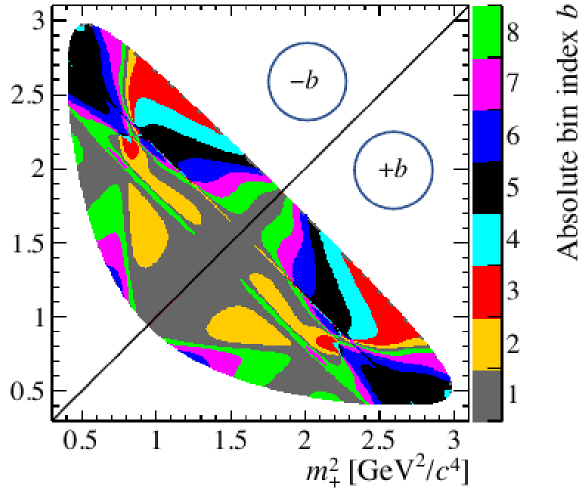

Simultaneous fit of the yield ratio $R_b^\pm$ ($\pm$ for initial $D^0/\bar{D}^0$) between $+b$ and $-b$ in bins of D^0 decay time t:

$$R_b^\pm(t) \approx r_b - \sqrt{r_b}[(1-r_b)c_b y - (1+r_b)s_b x]\Gamma t$$

- $r_b \equiv R_b(t=0)$
- c_b and s_b: parameters related to the strong phase differences between $\pm b$ regions (based on external inputs from CLEO and BESIII).

Mixing parameters in $\bar{B} \to D^0(\to K_S^0\pi^+\pi^-)\mu^-\bar{\nu}_\mu X$

Mixing measurement: $D^0 + \bar{D}^0$

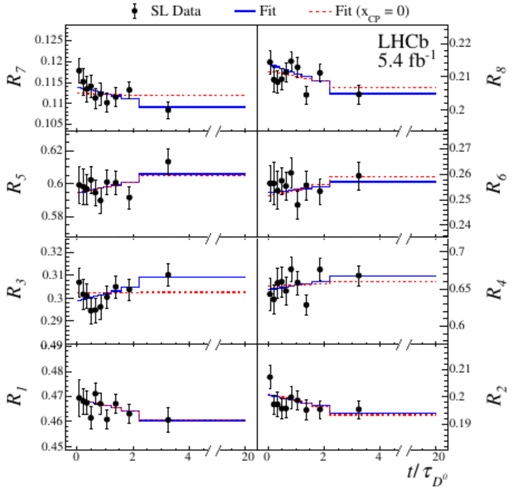

CPV measurement: $D^0 - \bar{D}^0$

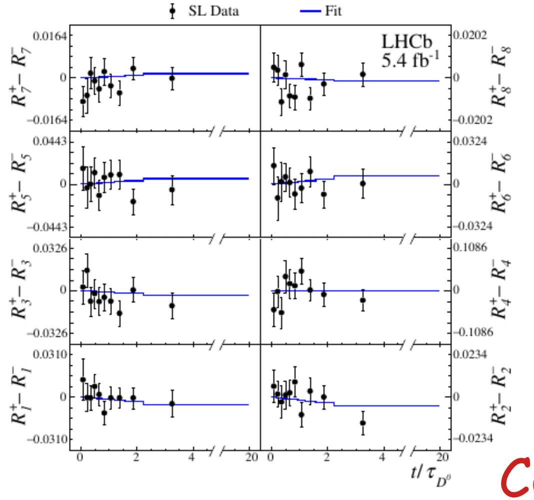

Summary of uncertainties

Source	x_{CP} $[10^{-3}]$	y_{CP} $[10^{-3}]$	Δx $[10^{-3}]$	Δy $[10^{-3}]$
Reconstruction and selection	0.06	0.79	0.28	0.24
Detection asymmetry	0.06	0.03	0.01	0.09
Mass-fit model	0.03	0.09	0.01	0.01
Unrelated $D^0\mu$ combinations	0.24	0.22	0.01	0.05
Total systematic	0.26	0.83	0.28	0.26
Strong phase inputs	0.32	0.68	0.16	0.21
Statistical (w/o phase inputs)	1.45	3.04	0.92	1.91
Statistical	1.48	3.12	0.93	1.92

Uncertainty on external strong phase inputs higher than total systematic → need for new BESIII inputs!

$$R_{bj}^{\pm} \approx \frac{r_b + \frac{1}{4} r_b \langle t^2\rangle_j \,\mathrm{Re}\left(z_{CP}^2 - \Delta z^2\right) + \frac{1}{4}\langle t^2\rangle_j \left|z_{CP} \pm \Delta z\right|^2 + \sqrt{r_b}\langle t\rangle_j \,\mathrm{Re}\left[X_b^*(z_{CP} \pm \Delta z)\right]}{1 + \frac{1}{4}\langle t^2\rangle_j \,\mathrm{Re}\left(z_{CP}^2 - \Delta z^2\right) + r_b \frac{1}{4}\langle t^2\rangle_j \left|z_{CP} \pm \Delta z\right|^2 + \sqrt{r_b}\langle t\rangle_j \,\mathrm{Re}\left[X_b(z_{CP} \pm \Delta z)\right]}$$

$$x_{CP} = -\,\mathrm{Im}\,(z_{CP}), \quad \Delta x = -\,\mathrm{Im}\,(\Delta z)$$
$$y_{CP} = -\,\mathrm{Re}\,(z_{CP}), \quad \Delta y = -\,\mathrm{Re}\,(\Delta z)$$

Combination of prompt and semileptonic analyses

$$x = (4.01 \pm 0.49) \times 10^{-3}$$
$$y = (5.50 \pm 1.30) \times 10^{-3}$$
$$|q/p| = 1.012^{+0.050}_{-0.048}$$
$$\phi = -0.060^{+0.037}_{-0.044}$$

Compatible results for prompt & SL

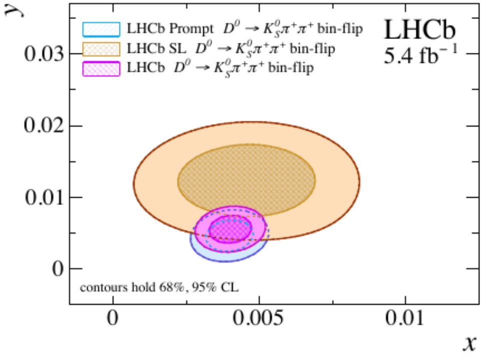

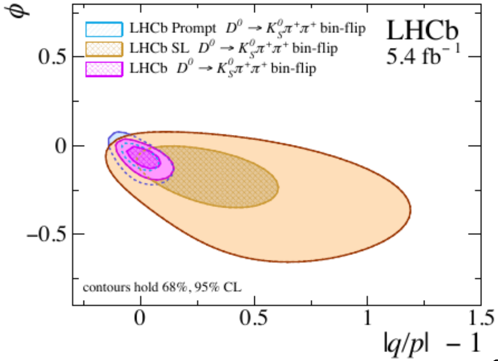

New combinations on charm mixing

- With respect to last ones, improvement of y by 40% thanks to new $y_{CP} - y_{CP}^{K\pi}$ result
- $\delta_D^{K\pi} \neq 180^{\circ}$ @ 3.6σ → Evidence of U-spin symmetry breaking
  - External inputs including BESIII measurement on strong-phase difference [EPJC 82 (2022) 1009]

$$x = (0.398^{+0.050}_{-0.049})\%$$

$$y = (0.636^{+0.020}_{-0.019})\%$$

$$r_D^{K\pi} = \frac{\mathcal{B}(D^0 \to K^+\pi^-, t=0)}{\mathcal{B}(D^0 \to K^-\pi^+, t=0)} = (5.865^{+0.014}_{-0.015})\%$$

$$\delta_D^{K\pi} = (190.2 \pm 2.8)^{\circ}$$

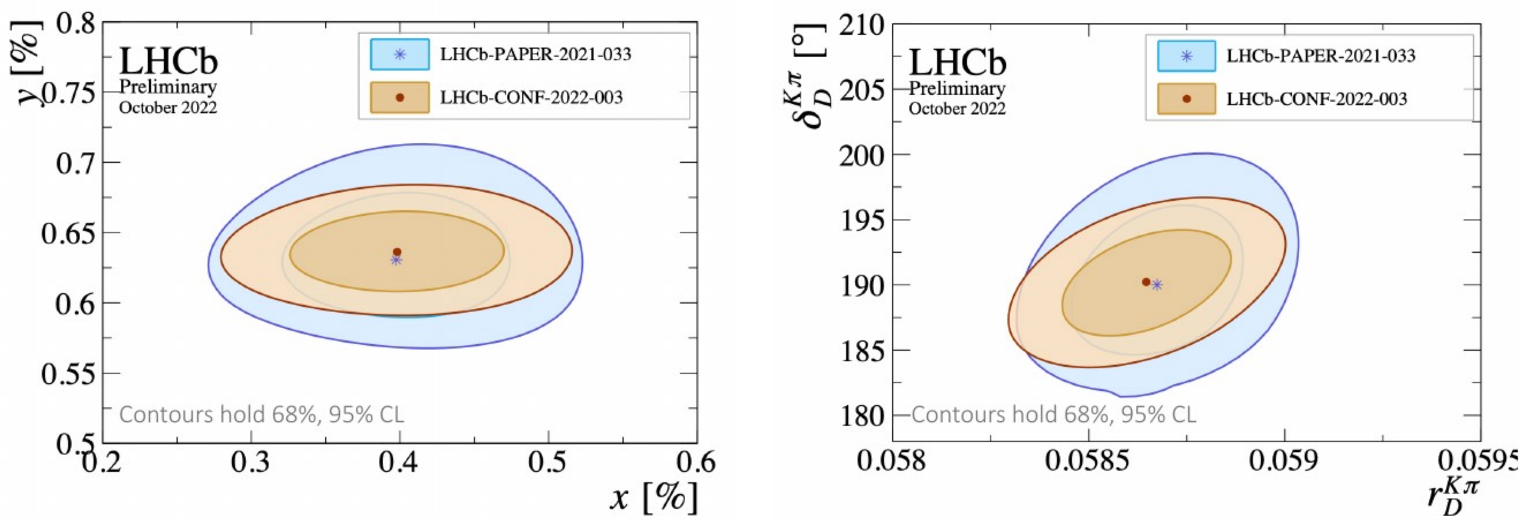

Please see Shunan's talk in the morning on y combination

[LHCb-CONF-2022-003]

New combinations on charm mixing

- With respect to last ones, improvement of y by 40% thanks to new $y_{CP} - y_{CP}^{K\pi}$ result
- $\delta_D^{K\pi} \neq 180^{\circ}$ @ 3.6σ → Evidence of U-spin symmetry breaking
  - External inputs including BESIII measurement on strong-phase difference [EPJC 82 (2022) 1009]

$$x = \left(0.398^{+0.050}_{-0.049}\right)\%$$

$$y = \left(0.636^{+0.020}_{-0.019}\right)\%$$

$$r_D^{K\pi} = \frac{\mathcal{B}(D^0 \to K^+\pi^-, t=0)}{\mathcal{B}(D^0 \to K^-\pi^+, t=0)} = \left(5.865^{+0.014}_{-0.015}\right)\%$$

$$\delta_D^{K\pi} = (190.2 \pm 2.8)^{\circ}$$

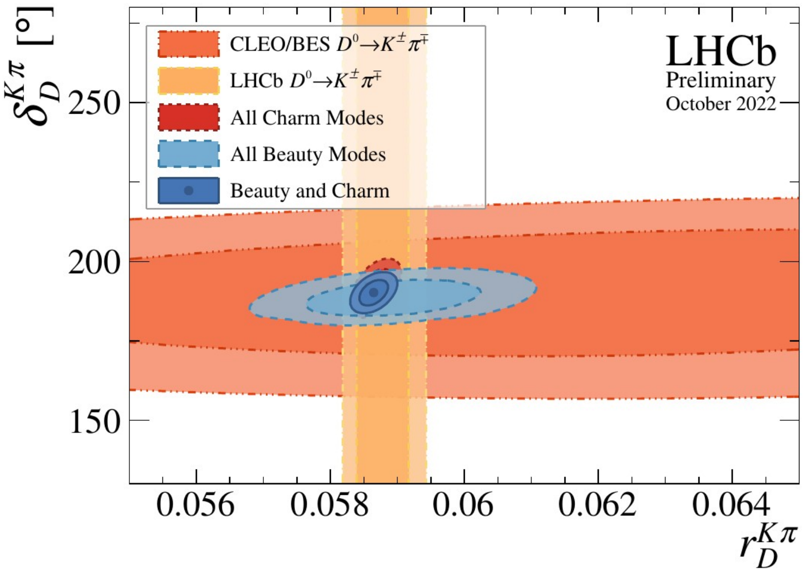

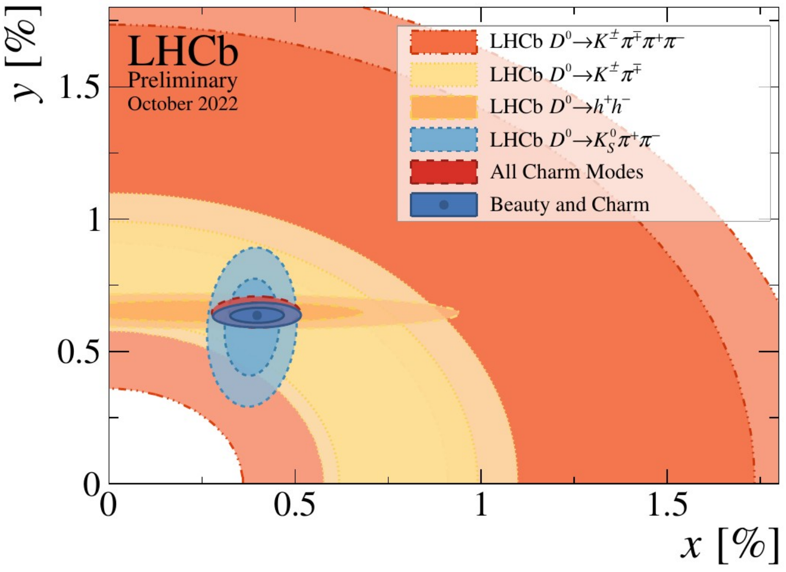

Amplitude analysis of $D_{(s)}^{+} \rightarrow \pi^{-}\pi^{+}\pi^{+}$

- 2012 data, $\mathcal{L} = 1.5\ \mathrm{fb}^{-1}$. Promptly produced D mesons

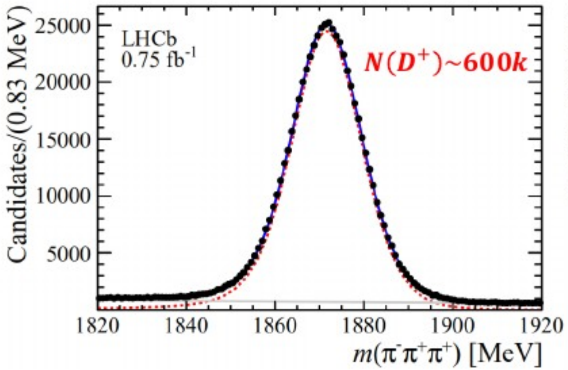

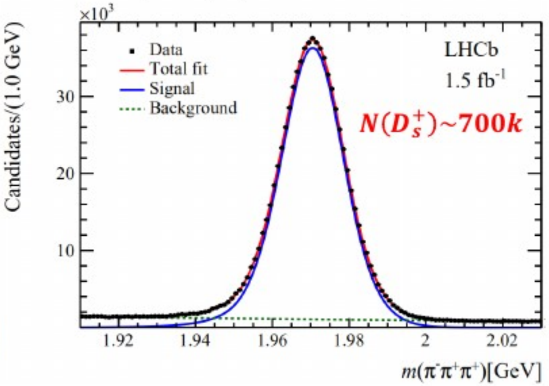

Statistics >50x prior measurements from $e^{+}e^{-}$ experiments & higher signal purity (BABAR/CLEO-c/BESIII)

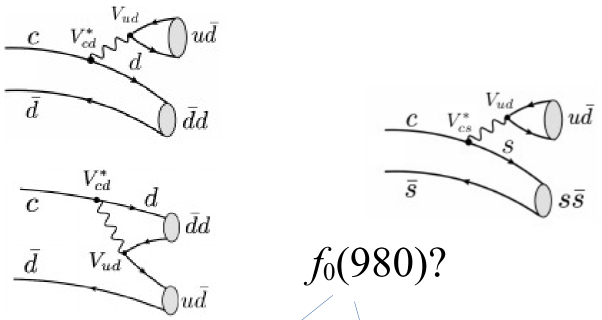

- **Competitive statistical power**

- Methodology for amplitude construction
  - **S-wave**: Quasi-Model Independent approach **(QMIPWA)**

$$\mathcal{A}_S(s_{12}, s_{13}) = \mathcal{A}_S(s_{12}) + \mathcal{A}_S(s_{13}) \qquad \mathcal{A}_S^k(s_{\pi^+\pi^-}) = c_k e^{i\phi_k}$$

    - c_k, ϕ_k: Generic functions determined by fit to data
  - **Isobar model for spin-1, spin-2 components**

$f_0(980)$?

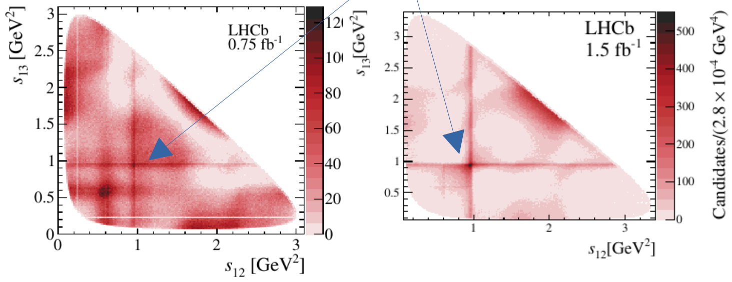

[arXiv:2208.03300, arXiv:2209.09840]

Amplitude analysis of $D_{(s)}^+ \to \pi^- \pi^+ \pi^+$

- $D^+ \to \pi^- \pi^+ \pi^+$

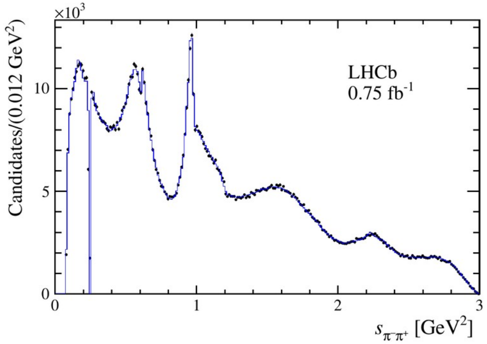

Component	Magnitude	Phase [°]	Fit fraction [%]
$\rho(770)^0\pi^+$	1 [fixed]	0 [fixed]	26.0 ± 0.3 ± 1.6 ± 0.3
$\omega(782)\pi^+$	$(1.68 \pm 0.06 \pm 0.15 \pm 0.02) \times 10^{-2}$	$-103.3 \pm 2.1 \pm 2.6 \pm 0.4$	$0.103 \pm 0.008 \pm 0.014 \pm 0.002$
$\rho(1450)^0\pi^+$	$2.66 \pm 0.07 \pm 0.24 \pm 0.22$	$47.0 \pm 1.5 \pm 5.5 \pm 4.1$	5.4 ± 0.4 ± 1.3 ± 0.8
$\rho(1700)^0\pi^+$	$7.41 \pm 0.18 \pm 0.47 \pm 0.71$	$-65.7 \pm 1.5 \pm 3.8 \pm 4.6$	5.7 ± 0.5 ± 1.0 ± 1.0
$f_2(1270)\pi^+$	$2.16 \pm 0.02 \pm 0.10 \pm 0.02$	$-100.9 \pm 0.7 \pm 2.0 \pm 0.4$	13.8 ± 0.2 ± 0.4 ± 0.2
S-wave			61.8 ± 0.5 ± 0.6 ± 0.5
$\sum_i \mathrm{FF}_i$			112.8
χ^2/ndof (range)	[1.47 - 1.78]		$-2\log\mathcal{L} = 805622$

Dominated by S-wave, followed by $\rho(770)^0\pi^+$ and $f_2(1270)^0\pi^+$

Contribution from $(\omega(782) \to \pi^+\pi^-)\pi^+$ observed for the first time

- $D_s^+ \to \pi^- \pi^+ \pi^+$

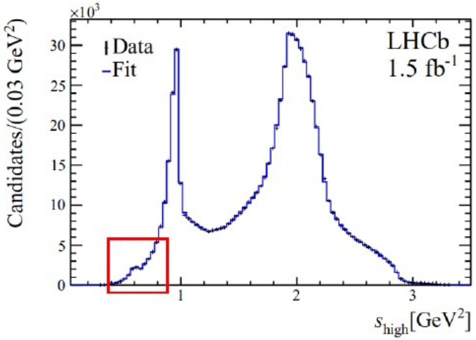

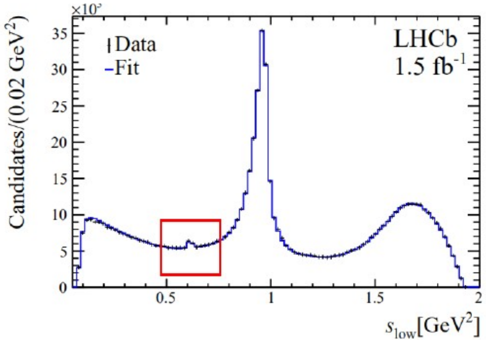

Also new!

Resonance	Magnitude	Phase [°]	Fit fraction (FF) [%]
S-wave			84.97 ± 0.14
$\rho(770)^0$	0.1201 ± 0.0030	79.4 ± 1.8	1.038 ± 0.054
$\omega(782)$	0.04001 ± 0.00090	-109.9 ± 1.7	0.360 ± 0.016
$\rho(1450)^0$	1.277 ± 0.026	-115.2 ± 2.6	3.86 ± 0.15
$\rho(1700)^0$	0.873 ± 0.061	-60.9 ± 6.1	0.365 ± 0.050
combined	–	–	6.14 ± 0.27
$f_2(1270)$	1 (fixed)	0 (fixed)	13.69 ± 0.14
$f_2'(1525)$	0.1098 ± 0.0069	178.1 ± 4.2	0.0455 ± 0.0070
sum of fit fractions			104.3
χ^2/ndof (range)	$[1.45 - 1.57]$		

Dominated by S-wave, followed by spin-2 resonances

Contribution from $(\omega(782) \to \pi^+\pi^-)\pi^+$observed for the first time

[arXiv:2208.03300, arXiv:2209.09840]

S-wave of $D_{(s)}^{+} \to \pi^{-}\pi^{+}\pi^{+}$

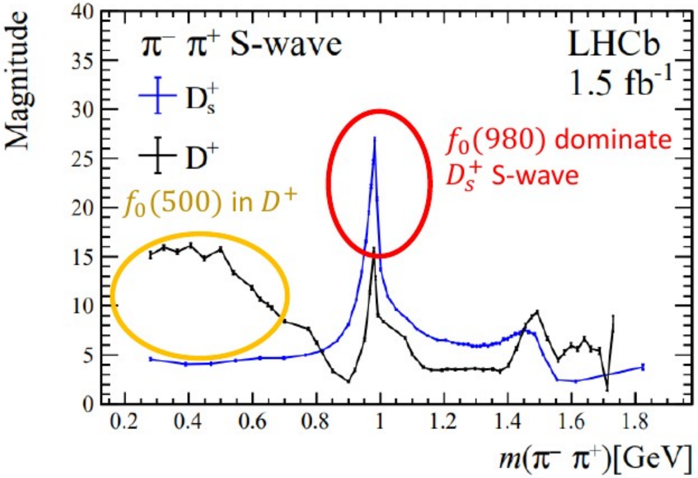

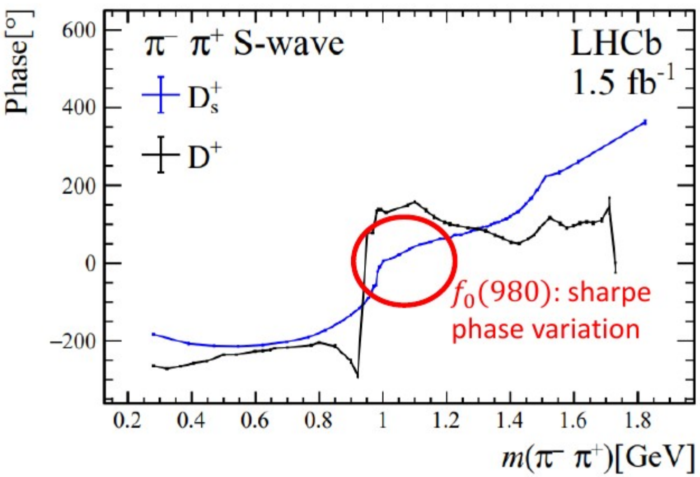

MIPWA results:

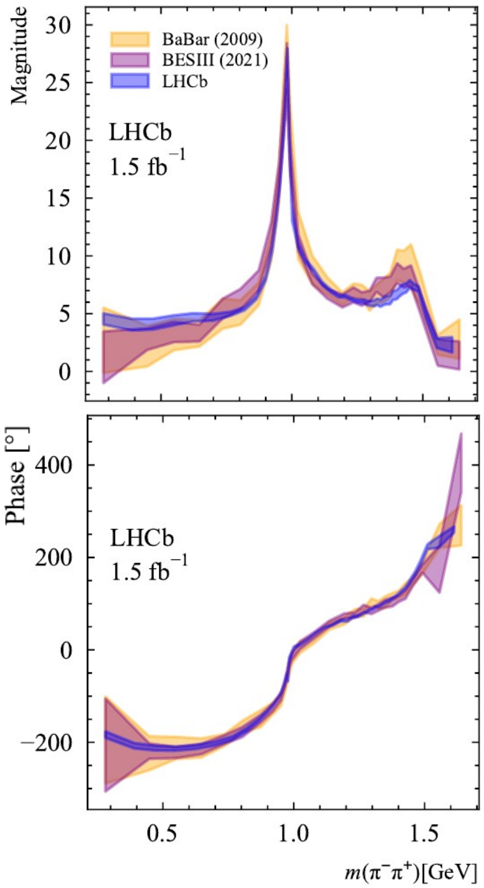

unitary chiral model, Int. J. Mod. Phys. **25**(2016)1630001

- Potential interpretation of the difference:

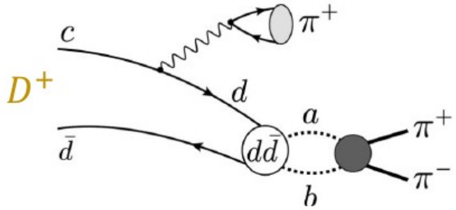

$$\sum_i d\bar{q}_i q_i \bar{d} = \underline{\pi^+\pi^- + \tfrac{1}{2}\pi^0\pi^0} - \tfrac{2}{\sqrt{6}}\pi^0\eta + K^0\overline{K}^0 + \tfrac{1}{3}\eta\eta$$

Indicating $f_0(500)$ as dynamical pole of $\pi\pi \to \pi\pi$ rescattering ?

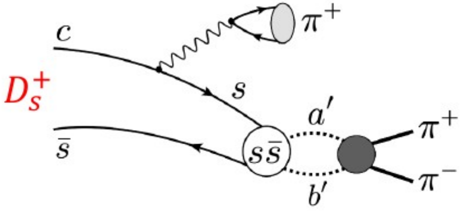

$$\sum_i s\bar{q}_i q_i \bar{s} = \underline{K^+K^- + K^0\overline{K}^0} + \tfrac{1}{3}\eta\eta$$

$f_0(980)$ strongly couples to KK channel

[arXiv:2208.03262, accepted by PRD]

Amplitude analysis of $\Lambda_c^+ \to pK^-\pi^+$

- 2016 data, $\mathcal{L} = 0.5\mathrm{fb}^{-1}$; ~400k signals; helicity-based Am.An.

Resonance	J^P	Mass (MeV)	Width (MeV)
$\Lambda(1405)$	$1/2^-$	1405.1	50.5
$\Lambda(1520)$	$3/2^-$	$1515-1523$	$10-20$
$\Lambda(1600)$	$1/2^+$	1630	250
$\Lambda(1670)$	$1/2^-$	1670	30
$\Lambda(1690)$	$3/2^-$	1690	70
$\Lambda(2000)$	$1/2^-$	$1900-2100$	$20-400$
$\Delta(1232)^{++}$	$3/2^+$	1232	117
$\Delta(1600)^{++}$	$3/2^+$	1640	300
$\Delta(1700)^{++}$	$3/2^-$	1690	380
$K_0^*(700)$	0^+	824	478
$K^*(892)$	1^-	895.5	47.3
$K_0^*(1430)$	0^+	1375	190

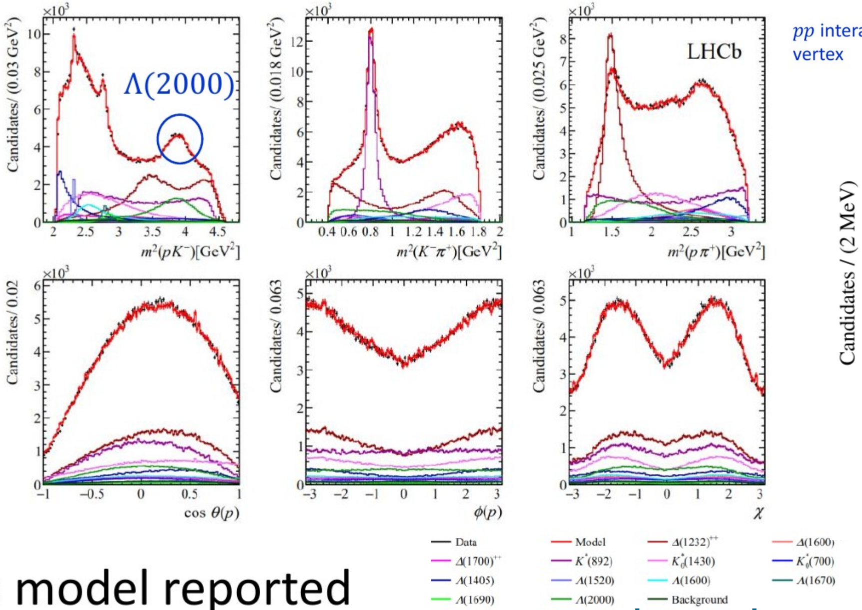

Decay orientation angles in the lab system

Λ_c^+ from b-hadron decays

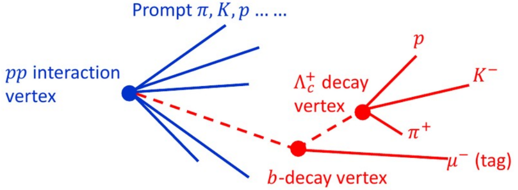

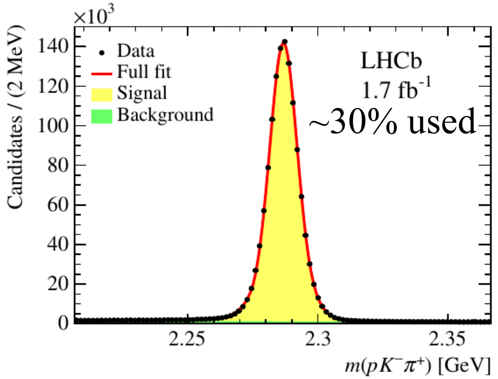

- All parameters of amplitude model reported
- Mass and width of $\Lambda(2000)$ determined

$$m = 1988 \pm 2 \pm 21\,\mathrm{MeV} \qquad \Gamma = 179 \pm 4 \pm 16\,\mathrm{MeV}$$

Λ_c^+ polarization measurement

$$p(\Omega, \boldsymbol{P}) = \frac{1}{\mathcal{N}} \sum_{m_p=\pm 1/2} \Big\{ (1 + \boxed{P_z}) |\mathcal{A}_{1/2,m_p}(\Omega)|^2 + (1 - \boxed{P_z}) |\mathcal{A}_{-1/2,m_p}(\Omega)|^2 + 2\mathrm{Re}\left[(\boxed{P_x} - \boxed{iP_y}) \mathcal{A}^*_{1/2,m_p}(\Omega) \mathcal{A}_{-1/2,m_p}(\Omega) \right] \Big\},$$

$$\Omega = (m^2_{pK^-}, m^2_{K^-\pi^+}, \cos\theta_p, \phi_p, \chi)$$

Final-state kinematics

Initial spin structure of Λ_c^+

- Large interference improves sensitivity to initial polarization

Advances in High Energy Physics (2020) 7463073

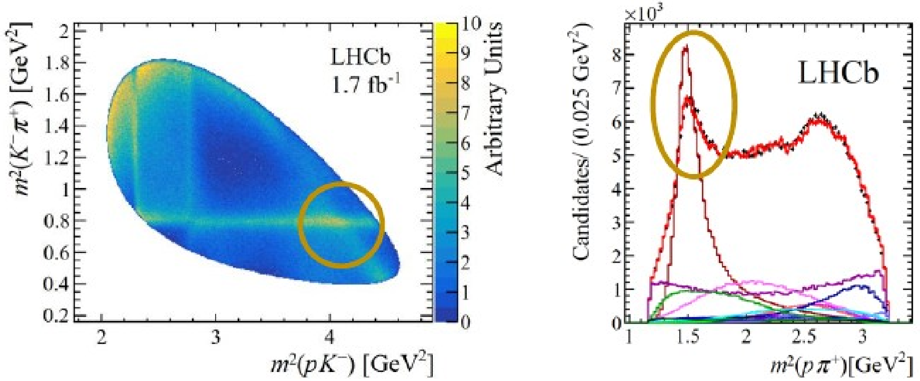

Large interference between $\Delta(1232)^{++}$ and $K^*(892)$

Λ_c^+ polarization from semileptonic b-decays measured, with 2 different definitions of initial spin axis

Model dependency contributes to the **largest syst.** uncertainty (second term)

Measured polarization $\boldsymbol{P}$ components

Component	Value (%)
P_x (*lab*)	$60.32 \pm 0.68 \pm 0.98 \pm 0.21$
P_y (*lab*)	$-0.41 \pm 0.61 \pm 0.16 \pm 0.07$
P_z (*lab*)	$-24.7 \pm 0.6 \pm 0.3 \pm 1.1$
P_x ($\tilde{B}$)	$21.65 \pm 0.68 \pm 0.36 \pm 0.15$
P_y ($\tilde{B}$)	$1.08 \pm 0.61 \pm 0.09 \pm 0.08$
P_z ($\tilde{B}$)	$-66.5 \pm 0.6 \pm 1.1 \pm 0.1$

Polarimeter vector field of $\Lambda_c^+ \to pK^-\pi^+$

$$|\mathcal{M}(\phi,\theta,\chi,\tau)|^2 = I_0(\tau)\left(1 + \sum_{i,j=1}^{3} P_i R_{ij}(\phi,\theta,\chi)\,\alpha_j(\tau)\right)$$

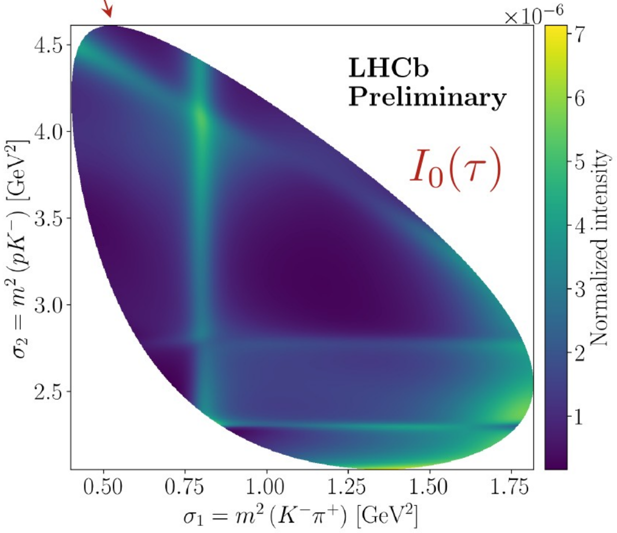

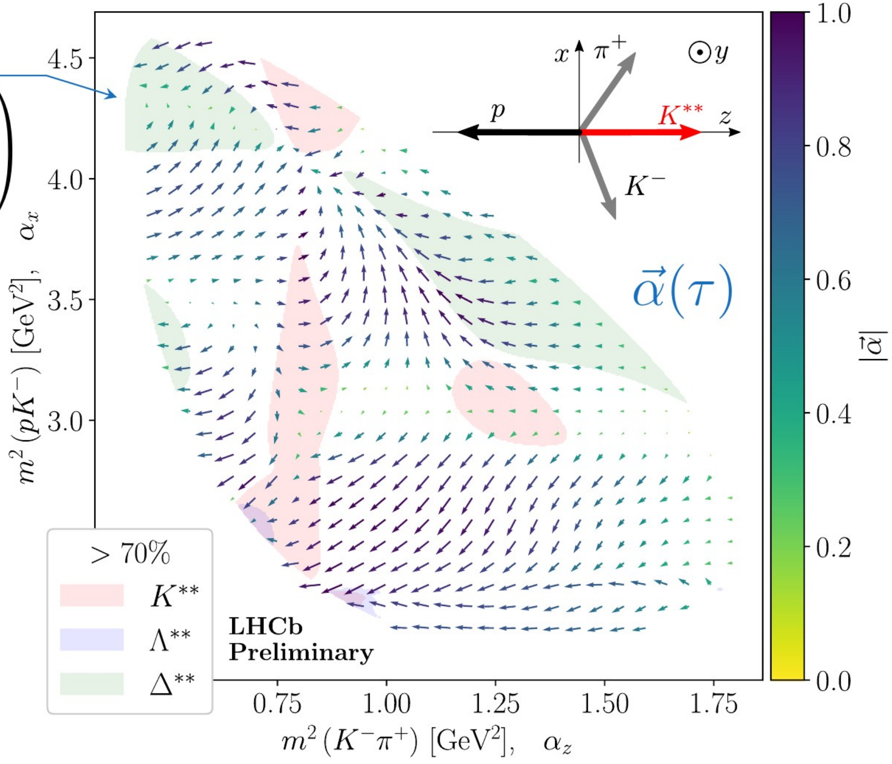

Important inputs for analyses involving Λ_c^+ [Details]

Searching for $D^0 \to \mu^- \mu^+$

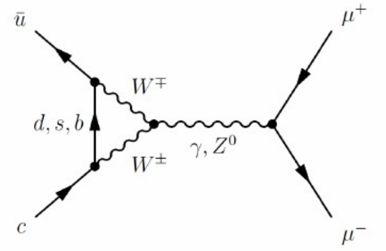

- FCNC & helicity suppression
- Predictions: $\mathcal{B}^{s.d.}(D^0 \to \mu^+\mu^-) \sim 10^{-18}$
  $\mathcal{B}^{(\gamma\gamma)}(D^0 \to \mu^+\mu^-) < 2.3 \times 10^{-11}$
- Full Run1+2 analysis (9 fb^{-1}), D^0 from prompt $D^{*+} \to D^0\pi^+_{tag}$
- Normalization channel: $\mathcal{B}(D^0 \to \mu^+\mu^-) = \alpha N_{D^0\to\mu^+\mu^-}, \quad \alpha \sim \frac{\mathcal{B}(D^0\to h^-\pi^+)}{N_{D^0\to h^-\pi^+}} \frac{\varepsilon_{D^0\to h^-\pi^+}}{\varepsilon_{D^0\to\mu^+\mu^-}} \sim 2 \times 10^{-11}$
- 2D simultaneous fits in 3 BDT bins per run:

Peaking mostly from π/μ misID

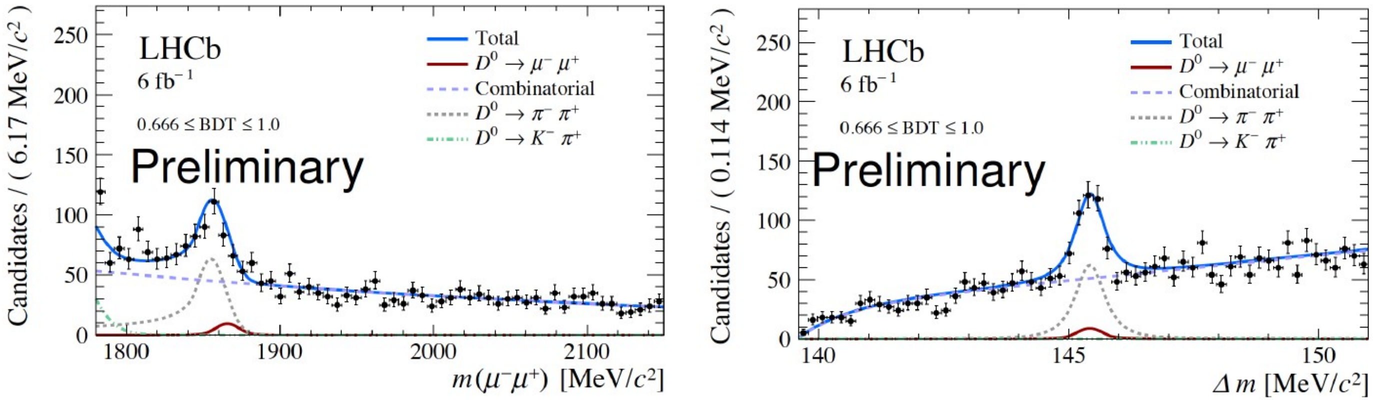

- Preliminary result:

$$\boxed{\mathcal{B}(D^0 \to \mu^+\mu^-) < 2.9(3.3) \times 10^{-9} \text{ at } 90(95)\% \text{ C.L.}}$$

Improvement of more a factor of two!

Summary & outlook

- LHCb is in fact a charm factory and has the world's largest samples of charm hadronic decays
- High statistics and superb detector performance allow for high precision measurements on charm mixing & CP, amplitude analyses, rare decays, etc.
- Still more charm results in the pipeline with full Run1+2 data, stay tuned!
  - More CPV observables, dielectron modes, SL decays, radiative, etc.
- Longer term: Run3 has started
- Synergy with BESIII important for mixing & CPV in the charm sector

Backup Slides

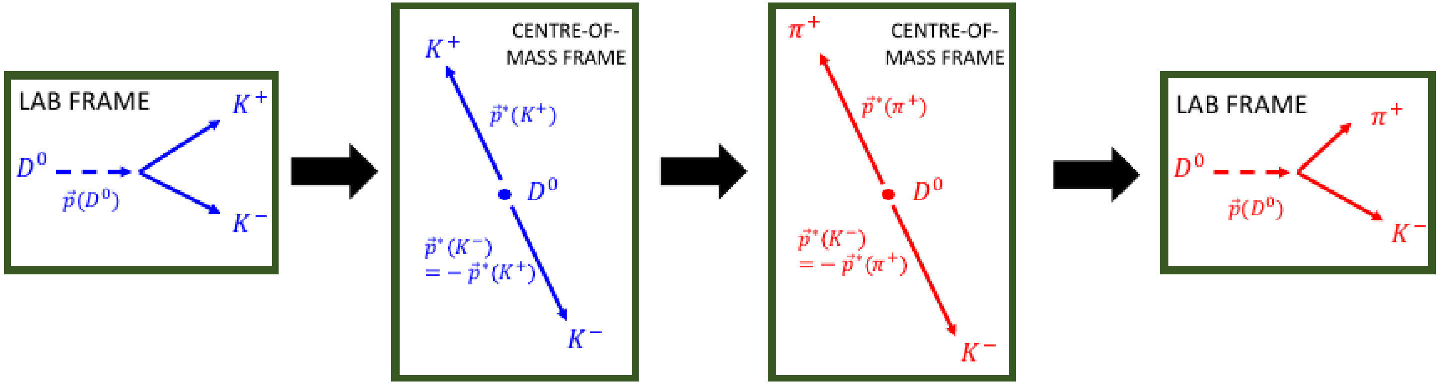

Figure 1: Sketch of a $D^0 \to K^-K^+$ to $D^0 \to K^-\pi^+$ matching.

$$|\vec{p}^*| = \frac{\sqrt{(m_{D^0}^2 - (m_{K^+} - m_{K^-})^2)(m_{D^0}^2 - (m_{K^+} + m_{K^-})^2)}}{2m_{D^0}}$$

[LHCb-CONF-2022-003]

B decay	D decay	Ref.	Dataset	Status since Ref. [14]
$B^{\pm} \to Dh^{\pm}$	$D \to h^+h^-$	[29]	Run 1&2	As before
$B^{\pm} \to Dh^{\pm}$	$D \to h^+\pi^-\pi^+\pi^-$	[30]	Run 1	As before
$B^{\pm} \to Dh^{\pm}$	$D \to K^{\pm}\pi^{\mp}\pi^+\pi^-$	[18]	Run 1&2	**New**
$B^{\pm} \to Dh^{\pm}$	$D \to h^+h^-\pi^0$	[19]	Run 1&2	**Updated**
$B^{\pm} \to Dh^{\pm}$	$D \to K^0_S h^+h^-$	[31]	Run 1&2	As before
$B^{\pm} \to Dh^{\pm}$	$D \to K^0_S K^{\pm}\pi^{\mp}$	[32]	Run 1&2	As before
$B^{\pm} \to D^* h^{\pm}$	$D \to h^+h^-$	[29]	Run 1&2	As before
$B^{\pm} \to DK^{*\pm}$	$D \to h^+h^-$	[33]	Run 1&2(*)	As before
$B^{\pm} \to DK^{*\pm}$	$D \to h^+\pi^-\pi^+\pi^-$	[33]	Run 1&2(*)	As before
$B^{\pm} \to Dh^{\pm}\pi^+\pi^-$	$D \to h^+h^-$	[34]	Run 1	As before
$B^0 \to DK^{*0}$	$D \to h^+h^-$	[35]	Run 1&2(*)	As before
$B^0 \to DK^{*0}$	$D \to h^+\pi^-\pi^+\pi^-$	[35]	Run 1&2(*)	As before
$B^0 \to DK^{*0}$	$D \to K^0_S\pi^+\pi^-$	[36]	Run 1	As before
$B^0 \to D^{\mp}\pi^{\pm}$	$D^+ \to K^-\pi^+\pi^+$	[37]	Run 1	As before
$B^0_s \to D_s^{\mp}K^{\pm}$	$D_s^+ \to h^+h^-\pi^+$	[38]	Run 1	As before
$B^0_s \to D_s^{\mp}K^{\pm}\pi^+\pi^-$	$D_s^+ \to h^+h^-\pi^+$	[39]	Run 1&2	As before
D decay	**Observable(s)**	**Ref.**	**Dataset**	**Status since Ref. [14]**
$D^0 \to h^+h^-$	ΔA_{CP}	[24, 40, 41]	Run 1&2	As before
$D^0 \to K^+K^-$	$A_{CP}(K^+K^-)$	[16, 24, 25]	Run 2	**New**
$D^0 \to h^+h^-$	$y_{CP} - y_{CP}^{K^-\pi^+}$	[42]	Run 1	As before
$D^0 \to h^+h^-$	$y_{CP} - y_{CP}^{K^-\pi^+}$	[15]	Run 2	**New**
$D^0 \to h^+h^-$	ΔY	[43–46]	Run 1&2	As before
$D^0 \to K^+\pi^-$ (Single Tag)	$R^{\pm}$, $(x'^{\pm})^2$, $y'^{\pm}$	[47]	Run 1	As before
$D^0 \to K^+\pi^-$ (Double Tag)	$R^{\pm}$, $(x'^{\pm})^2$, $y'^{\pm}$	[48]	Run 1&2(*)	As before
$D^0 \to K^{\pm}\pi^{\mp}\pi^+\pi^-$	$(x^2+y^2)/4$	[49]	Run 1	As before
$D^0 \to K^0_S\pi^+\pi^-$	x, y	[50]	Run 1	As before
$D^0 \to K^0_S\pi^+\pi^-$	x_{CP}, y_{CP}, Δx, Δy	[51]	Run 1	As before
$D^0 \to K^0_S\pi^+\pi^-$	x_{CP}, y_{CP}, Δx, Δy	[52]	Run 2	As before
$D^0 \to K^0_S\pi^+\pi^-$ (μ^- tag)	x_{CP}, y_{CP}, Δx, Δy	[17]	Run 2	**New**

[arXiv:2208.03300]

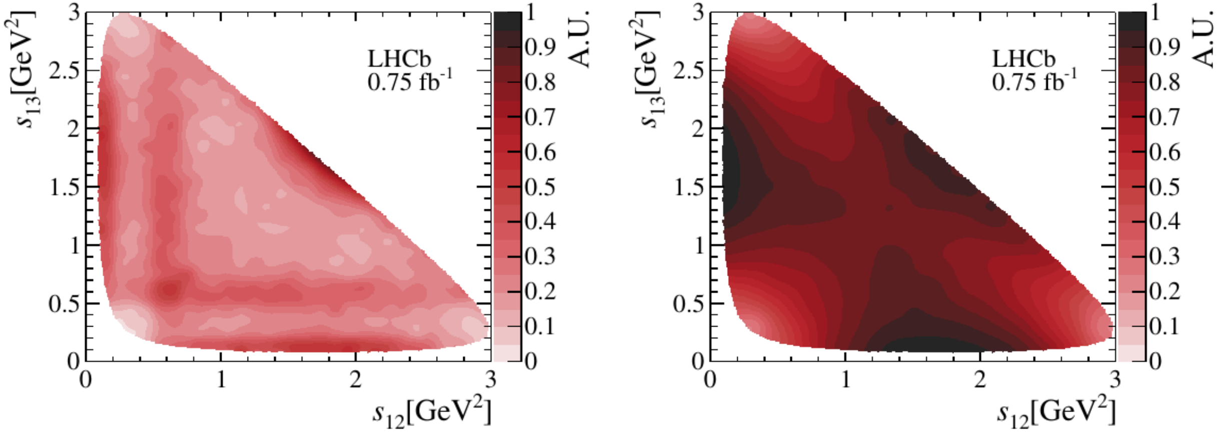

Amplitude analysis of the $D^+ \to \pi^-\pi^+\pi^+$ decay and measurement of the $\pi^-\pi^+$ S-wave amplitude

Figure 4: Models for (left) background distribution and (right) signal efficiency across the Dalitz plot, where the z-axis scale is arbitrary.

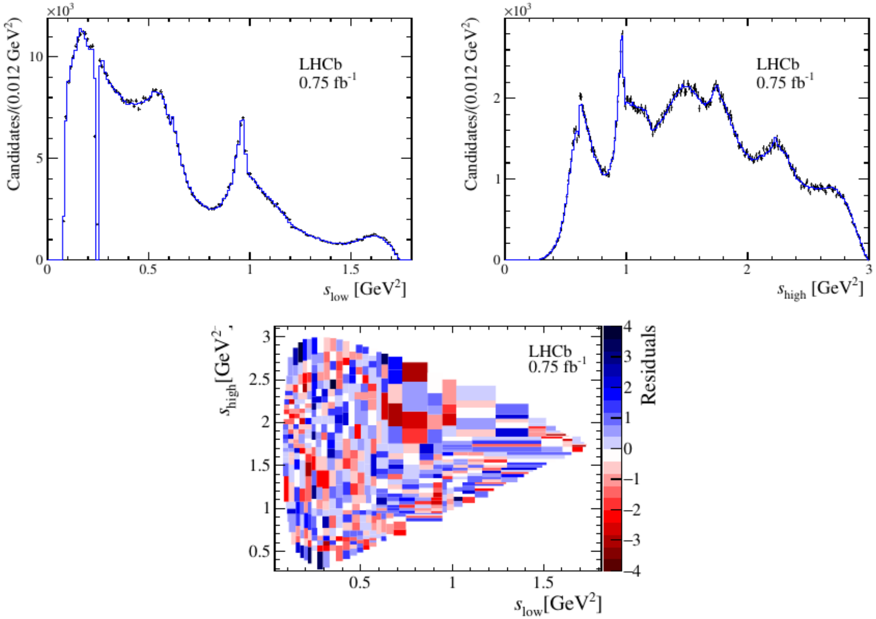

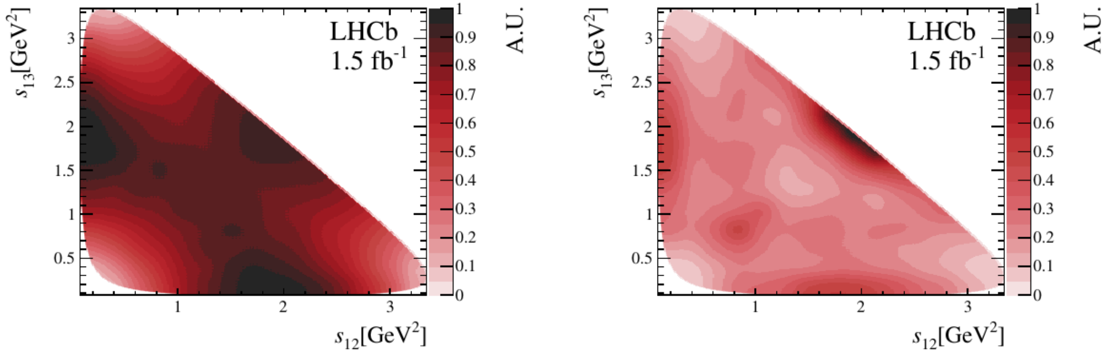

Figure 4: (Left) efficiency variation over the Dalitz plot and (right) background model for $D_s^+ \to \pi^-\pi^+\pi^+$ decays.

Amplitude analysis of the $D_s^+ \to \pi^-\pi^+\pi^+$ decay

mode	this result	BaBar	BESIII
S-wave	84.97 ± 0.64	83.0 ± 2.1	84.2 ± 1.4
$\rho(770)^0\pi^+$	1.04 ± 0.12	1.8 ± 1.1	0.9 ± 0.8
$\omega(782)\pi^+$	0.360 ± 0.022	–	–
$\rho(1450)^0\pi^+$	3.86 ± 2.0	2.3 ± 1.9	1.3 ± 0.8
$\rho(1700)^0\pi^+$	0.37 ± 0.34	–	–
$f_2(1270)\pi^+$	13.60 ± 0.50	10.1 ± 1.9	10.5 ± 1.4
$f_2'(1525)\pi^+$	0.045 ± 0.011	–	–

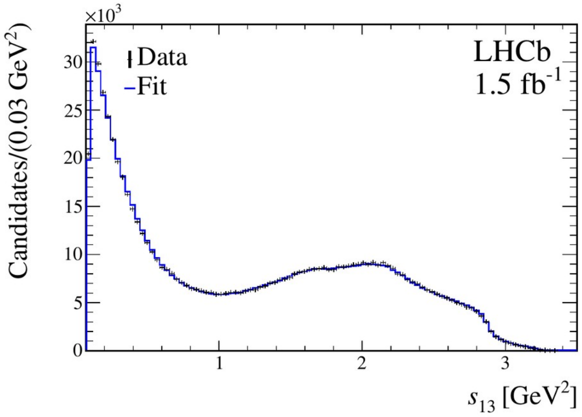

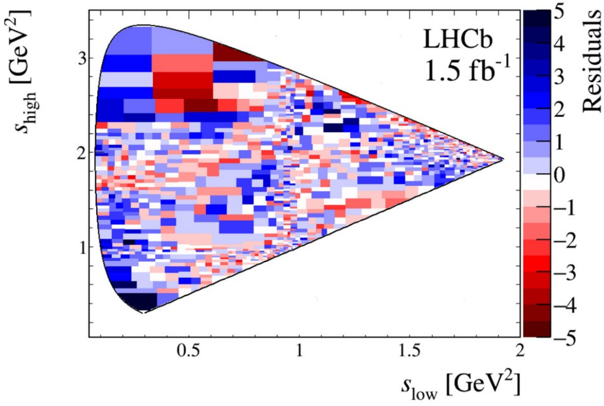

Λ_c^+ polarization frame

- Polarization measured in two Λ_c^+ helicity rest frames, with orthogonal components defined from the muon direction

- Laboratory frame: no reconstruction uncertainties
- Approximate B rest frame: closer to semileptonic decay physics

$$\hat{\boldsymbol{z}}_{\Lambda_c^+} = \hat{\boldsymbol{p}}(\Lambda_c^+)$$

$$\hat{\boldsymbol{x}}_{\Lambda_c^+} = \frac{\boldsymbol{p}(\Lambda_c^+) \times \boldsymbol{p}(\mu^-)}{|\boldsymbol{p}(\Lambda_c^+) \times \boldsymbol{p}(\mu^-)|} \times \hat{\boldsymbol{p}}(\Lambda_c^+)$$

$$\hat{\boldsymbol{y}}_{\Lambda_c^+} = \hat{\boldsymbol{z}}_{\Lambda_c^+} \times \hat{\boldsymbol{x}}_{\Lambda_c^+}$$

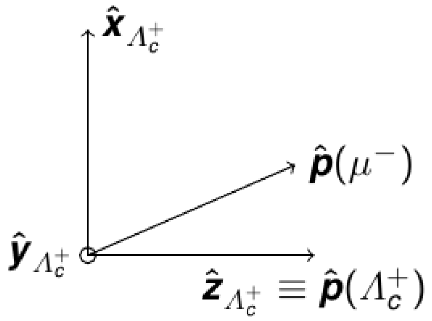

- Longitudinal (P_z) and transverse (P_x) polarisation are T-even, while normal (P_y) polarisation is T-odd
- P_y can be produced only by T-violation or (EM) final state interactions, see Sozzi, *Discrete symmetries and CPV*

$\Xi_c^+ \to pK^-\pi^+$ SL amplitude analysis ongoing

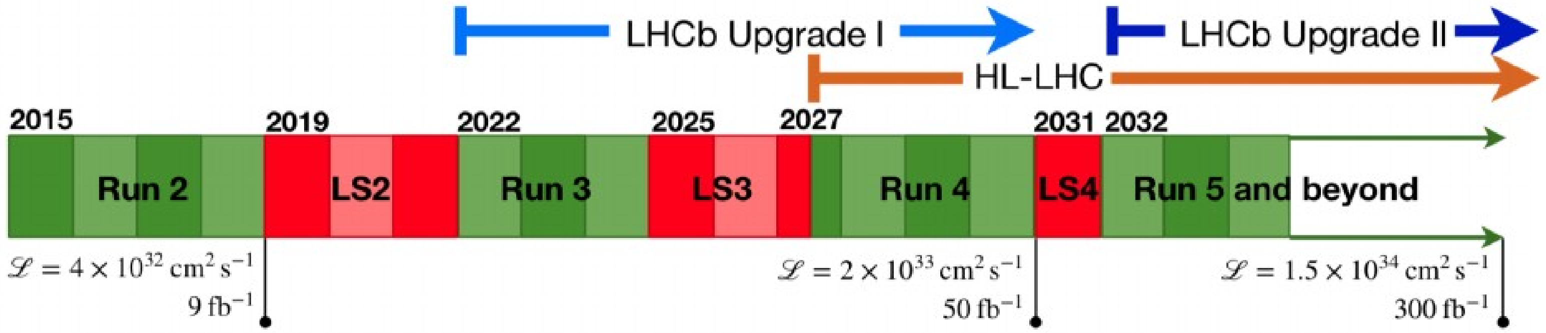

	Mode	Upgrade (50 fb^{-1})	Upgrade II (300 fb^{-1})
Limits on BFs	$D^0 \to \mu^+\mu^-$	4.2×10^{-10}	1.3×10^{-10}
	$D^+ \to \pi^+\mu^+\mu^-$	10^{-8}	3×10^{-9}
	$D_s^+ \to K^+\mu^+\mu^-$	10^{-8}	3×10^{-9}
	$\Lambda_c^+ \to p\mu^+\mu^-$	1.1×10^{-8}	4.4×10^{-9}
	$D^0 \to e\mu$	10^{-9}	4.1×10^{-9}
Stat. precision on asymmetries	$D^+ \to \pi^+\mu^+\mu^-$	0.2%	0.08%
	$D^0 \to \pi^+\pi^-\mu^+\mu^-$	1%	0.4%
	$D^0 \to \pi^+K^-\mu^+\mu^-$	0.3%	0.13%
	$D^0 \to K^+\pi^-\mu^+\mu^-$	12%	5%
	$D^0 \to K^+K^-\mu^+\mu^-$	4%	1.7%